Features of a Reattaching Turbulent Shear Layer in Divergent Channel Flow

David M. Driver* and H. Lee Seegmiller*
NASA Ames Research Center, Moffett Field, California

Experimental data have been obtained in an incompressible turbulent flow over a rearward-facing step in a diverging channel flow. Mean velocities, Reynolds stresses, and triple products that were measured by a laser Doppler velocimeter are presented for two cases of tunnel wall divergence. Eddy viscosities, production, convection, turbulent diffusion, and dissipation (balance of kinetic energy equation) terms are extracted from the data. These data are compared with various eddy-viscosity turbulence models. Numerical calculations incorporating the k-ϵ and algebraic-stress turbulence models are compared with the data. When determining quantities of engineering interest, the modified algebraic-stress model (ASM) is a significant improvement over the unmodified ASM and the unmodified k-ϵ model; however, like the others, it dramatically overpredicts the experimentally determined dissipation rate.

Nomenclature

C_f = wall skin-friction coefficient, $\tau_w/(\frac{1}{2}\rho U_{\text{ref}}^2)$
C_p = wall static pressure coefficient, $(P_w - P_{\text{ref}})/(\frac{1}{2}\rho_{\text{ref}} U_{\text{ref}}^2)$
H = step height
k = turbulent kinetic energy
M = Mach number
P = static pressure
Re = Reynolds number
U, V = mean velocity in X and Y directions, respectively
$\langle uk \rangle$ = turbulent correlation of kinetic energy in the X direction
$\langle u^2 \rangle, \langle v^2 \rangle, \langle w^2 \rangle$ = mean-square velocity fluctuation in X, Y, and spanwise directions, respectively
$\langle u^3 \rangle$ = turbulent triple-product correlation of u^2 in the X direction
$\langle uv \rangle$ = mean-square velocity fluctuation correlation
$\langle uv^2 \rangle$ = turbulent triple-product correlation of v^2 in the x direction
$\langle vk \rangle$ = turbulent correlation of kinetic energy in the Y direction
$\langle vu^2 \rangle$ = turbulent triple-product correlation of u^2 in the Y direction
$\langle v^3 \rangle$ = turbulent triple-product correlation of v^2 in the Y direction
X = streamwise coordinate parallel to model centerline measured from the edge of the step
Y = vertical coordinate normal to the step-side wall measured from the bottom of the step
Y_0 = tunnel height upstream of the step
α = opposite wall deflection angle, deg
δ = boundary-layer thickness
δ^* = displacement thickness, $\int_0^\delta (1 - U/U_e)\,dy$
ϵ = dissipation rate of kinetic energy
θ = momentum thickness, $\int_0^\delta (U/U_e)(1 - U/U_e)\,dy$
ν_m = molecular viscosity (1.5×10^{-5} m^2/s)
ν_t = turbulent eddy viscosity
ρ = density
τ = shear-stress
$\langle ( ) \rangle$ = ensemble average value

Subscripts

e = boundary-layer edge conditions
ref = reference station ($x/H = -4$) conditions
R = reattachment station conditions
w = wall

Superscript

$\bar{(\ )}$ = time average value

Received June 17, 1982; revision received March 22, 1984. This paper is declared a work of the U.S. Government and therefore is in the public domain.

*Research Scientist, Experimental Fluid Dynamics Branch.

Introduction

REATTACHMENT of separated turbulent shear layers in the presence of adverse pressure gradients occurs in many aerodynamic flows of interest; for example, flow on airfoils, in diffusers, and in cavities. Extensive separation, with the attendant lack of pressure recovery, leads to a loss in lift and an increase in drag; it is detrimental to the aerodynamic efficiency of a vehicle. In most practical situations, the reattaching shear layer is in the presence of a pressure gradient and occurs on a surface with complex geometry, making strong interaction between the separation and reattachment process likely. Independent study of either phenomenon by itself is therefore difficult. The rearward-facing step geometry offers one of the least complex separating and reattaching flows (fixed location of separation), facilitating a study of the reattachment process by itself.

Previous studies of pressure-gradient effects on rearward-facing step flows were limited to small gradients produced by the sudden expansion of the tunnel walls at the step.[1] Recent improvements in the prediction of the backward-facing step flow with little or no pressure gradient have stimulated interest in the effects of pressure gradient on the flow.[2] Kuehn[3] demonstrated that the reattachment process is very sensitive to pressure gradient. In contrast to Kuehn's results, turbulence models that successfully predict reattachment with little or no pressure gradient are relatively insensitive to the changes produced by large pressure gradients.[2] Therefore, further progress in turbulence modeling will require additional information from well-planned and detailed experiments before these more complex flows can be adequately predicted. In particular, there exists a need for detailed measurements in rearward-step flow experiments that will answer some of the following fundamental questions about turbulence modeling.

What is the role of dissipation in reattachment? How are the Reynolds stresses affected by pressure gradient? What are the deficiencies in the closure models?

This paper presents detailed measurements, analyses, and comparisons with numerical predictions of two cases of reattaching turbulent shear flow behind a two-dimensional rearward-facing step in a diverging channel flow. Diverging the walls produces an adverse pressure gradient on the reattached boundary layer; however, pressure gradient is reduced in the reattachment zone. The experiment was conducted in an incompressible, high-Reynolds-number flow. Channel divergence was accomplished by deflecting the wall opposite the step. A laser Doppler velocimeter (LDV) was used to obtain mean-velocity and turbulence measurements throughout the flowfield. A laser interferometer skin-friction apparatus was used to provide skin-friction measurements along the step-side wall through the separation zone. The experiment was used as a predictive case in the 1981 Stanford conference[2] for evaluating turbulence models and predictive methods. Turbulent kinetic energy production, convection, and transport by Reynolds stresses and dissipation (inferred from kinetic energy equation balance) have been extracted from the data and compared with turbulence models. These data should be useful in guiding turbulence modeling efforts.

Experiment

Test Configuration

The experiments were conducted on the tunnel floor of a low-speed wind tunnel facility (see Fig. 1). The test configuration consisted of a 1.0-m long × 15.1-cm wide × 10.1-cm high rectangular inlet duct followed by a 1.27-cm rearward-facing step in the floor. The wall opposite the step (opposite wall) is hinged at a location 0.6 cm upstream of the step, permitting the wall to be deflected and a pressure gradient to be imposed on the freestream. This test configuration has a large aspect ratio (tunnel-width-to-step-height ratio of 12) to minimize three-dimensional effects in the separated region,[4] and a small expansion ratio $[(Y_0 + H)/Y_0 = 1.125]$ to minimize the freestream pressure gradient owing to sudden expansion.[5]

The experiment was performed at a freestream velocity of 44.2 m/s and at atmospheric total pressure and temperature. These conditions correspond to a freestream Mach number of 0.128. The step-side wall boundary layer was tripped at a location 1.0 m upstream of the step with a strip of No. 60 grit sandpaper 12.5 cm long and 15.2 cm wide (full span). The wall boundary-layer thickness was 1.9 cm, and the Reynolds number (based on momentum thickness) was 5000 at a location 4 step-heights upstream of the step. This high Reynolds number was chosen to insure that the boundary layer would be fully turbulent before passing over the step.

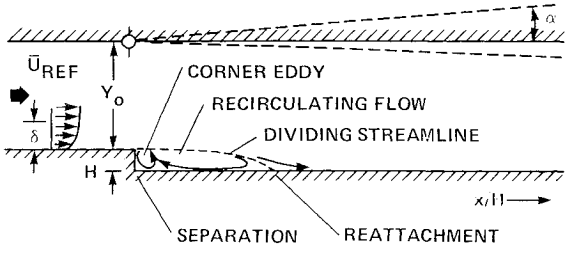

TUNNEL GEOMETRY: $H = 1.27$ cm, $y_o = 8H$
TUNNEL SPAN: 12H
TOP-WALL ANGLES: $-2° \leqslant \alpha \leqslant 10°$

INLET CONDITIONS: $U_{REF} = 44.2$ m/sec, $M_{REF} = 0.128$
$\delta_{BL} = 1.9$ cm, $Re_\theta = 5000$

Fig. 1 Rearward-facing step-flow experimental geometry and inlet conditions.

Two cases of wall divergence are studied in detail: 1) a parallel-wall case ($\alpha = 6$ deg) and 2) a deflected top-wall case ($\alpha = 6$ deg). The second case resulted in a 30% increase in reattachment length.

Surface and Flowfield Measurements

Wall static pressures were measured with 0.2-mm-diam orifices on tunnel centerline typically spaced every half-step height through the recirculating and reattachment zone. The uncertainties in measuring wall pressure led to an uncertainty in the wall static pressure coefficient of ± 0.009 (with 95% confidence limits).

Time-averaged surface skin-friction measurements of the step-side wall were made, using an oil-flow laser interferometer described in Refs. 6 and 7. A drop of oil on the floor (flowing due to skin friction) will reflect laser light at the air-oil interface and from the floor (after having passed through the oil). The two reflected beams are received at a photodiode where either constructive or destructive interference takes place (depending on the instantaneous path length of the two beams). The signal produced is a time record of the change in thickness of the oil on the surface, from which skin friction is inferred. Skin friction was measured along the step-side wall for both cases of opposite-wall deflection angles. Uncertainties in skin friction were assessed to be $\pm 8\%$ for a 95% confidence level (with an uncertainty of $\pm 15\%$ in the separated region of the flow).

To detect the instantaneous near-wall flow direction, two thermal-tuft probes were mounted in the vicinity of reattachment. The thermal-tuft wall probe (described in Ref. 8) employs a central heated wire and two sensor wires (lying parallel to the heated wire), one upstream and one downstream to detect the wake of the central heated wire. All three wires were located approximately 0.25 mm above the floor. The tungsten sensor wires were 0.005 mm in diameter, and the Monel heater wire was 0.125 mm in diameter. Spacing was 1.8 mm and the wires were 3.0 mm long. The resistances of the two sensor wires were compared in a bridge circuit to determine which of the two wires was the hottest, the bridge circuit being balanced before the heater wire was turned on. A positive bridge voltage indicated flow in the downstream direction, and a negative voltage indicated flow in the upstream direction. Time-averaging the signal (normalized by the absolute magnitude of the signal) gave intermittency (percent of time the flow direction was downstream). A probe was repositioned along the floor of the tunnel to locate the reattachment point as determined by 50% intermittency.

Measurements of mean velocities, Reynolds stresses, and turbulent triple products were obtained with a two-color laser Doppler velocimeter (LDV) described in Ref. 9. The 0.488 and 0.5145 μm wavelength beams of an argon-ion laser were used to produce two LDV fringe patterns with spacings of 4.48 and 4.57 μm. The measuring volume was estimated to be less than 0.3 mm in diameter and 1.0 mm long in the spanwise direction. Each of the two pairs of beams had one beam Bragg-shifted by 40 MHz to eliminate ambiguity of flow direction. The two channels of LDV were operated simultaneously with beams aligned at $+45$ and -45 deg to the axis of the tunnel for measurements of $U+V$ and $U-V$ components of velocity. Forward scattered light from particles passing through the measuring volume was detected by photomultiplier tubes. The signals from the photomultiplier tubes were processed in counters that performed five to eight periodicity checks on the signals and digitized the signals with 0.1-ns resolution.

Five channels of data were acquired for each valid LDV measurement. Two channels were of LDV velocity data, one channel was a time reading from a 100 kHz digital clock, and two channels were of flow direction data near the wall by two thermal tufts (one situated 9.5 mm upstream of reattachment and the other 9.5 mm downstream of reattachment). The two analog signals from the thermal tufts were digitized in an analog/digital converter and all five channels were multi-

plexed into the buffer of a high-speed digital minicomputer, which recorded the data on magnetic tape. To increase the frequency of measurements, the flow was seeded with 0.5 μm polystyrene spheres which were carried in an alcohol vapor into the plenum chamber of the tunnel. At each measurement station, more than 10,000 particles were observed and recorded at a rate that varied from 50 samples/s in the separated zone to 2000 samples/s at the outer edge of the boundary layer.

The mean velocities, Reynolds stresses, and turbulent triple products were determined by ensemble-averaging, without velocity bias corrections. Ensemble-averaging using a bias correction was determined to be inappropriate for this set of data.[10]

Two-Dimensionality of the Flowfield

Two-dimensionality of the mean flow was validated, based on oil flow patterns on the tunnel floor, observations of spanwise variations of certain flow quantities, and estimates of the two-dimensional momentum integral equation from the measured data.

Computations

A concurrent numerical study by Sindir and Launder under a NASA grant was undertaken for the purpose of developing turbulence models for predicting step flows. The investigators modified a version of the TEACH code[11] to accommodate a kinetic-energy dissipation rate (k-ϵ) turbulence model and an algebraic-stress turbulence model (ASM). The code solves the incompressible Navier-Stokes equations in two dimensions for three to five variables, using a control-volume approach and successive line overrelaxation. In order to achieve grid independence (determined by grid refinement tests), grid sizes of 42×42 for the undeflected-wall case and 42×52 for the 6 deg deflected-wall case were used.

The modeling study began by applying the k-ϵ model to predict an earlier flow over a larger step, as well as the flow studied by Kim et al.[12] The calculations by the k-ϵ model were generally poor, with reattachment severely underpredicted. The calculations were seen to overestimate eddy viscosity and consequently overpredicted turbulent shear-stress, causing the shear layer to spread too rapidly and the flow to reattach prematurely. This led Sindir and Launder to suspect that a k-ϵ model was inadequate and that maybe it was necessary to go to an ASM. Interestingly, the ASM produced very nearly the same results as the k-ϵ model, with only a slight improvement in reattachment length. Sindir and Launder then tried modifications to the dissipation rate equation of the ASM, since the equation was merely contrived by making it resemble the kinetic energy equation and requiring that the units be correct. They discovered that a modification of the production term in the dissipation rate equation resulted in a marked improvement. As a consequence of this modification, the turbulent shear-stress was brought into closer agreement with the earlier experiments; and the reattachment length, along with most other quantities of interest, was also improved. Surprisingly enough this same modification had little or no effect on the k-ϵ model prediction.

Sindir and Launder also applied these models to the two divergent wall cases of the present study (without prior knowledge of the experimental results). They submitted their results to the 1980-81 Stanford conference[2] where limited comparisons were made. The present paper includes preliminary comparisons of the data and calculations. Primarily, the ASM (mod-ϵ) results will be shown, since comparisons of the other models with severely shortened reattachments are difficult to assess. Details of Sindir's work will soon be published in a doctoral thesis.[13]

Results and Discussion

Flowfield measurements were made for 22 streamwise profiles for both test cases in an effort to facilitate taking streamwise derivatives of the data. The large number of profiles also demonstrates the self-consistency of the data, and gives a well-documented flow for turbulence modelers and code developers to attempt to calculate.

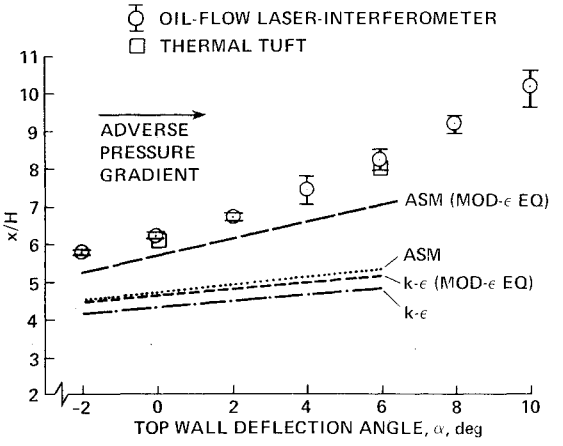

Fig. 2 Reattachment location vs top-wall deflection angle.

Reattachment Length

The reattachment length is a sensitive parameter that has historically been used to assess the overall predictive capability of turbulence models. In this experiment, the wall opposite the step is deflected to impose a pressure gradient on the freestream and thus significantly alter reattachment. The location of reattachment was inferred from a linear interpolation of the oil-flow laser skin-friction measurements. These results are plotted as a function of top-wall deflection angle (see Fig. 2). Uncertainty of reattachment location, as measured by this technique, is indicated by the bars on the data in Fig. 2. Also plotted are reattachment locations as determined by the thermal-tuft wall probes (50% intermittency). Excellent agreement is seen between both techniques of measuring reattachment. Also plotted are calculations made by Sindir,[13] using the ASM and the k-ϵ turbulence model with and without modifications to the divergence of the wall opposite to the step. The calculations demonstrate the significant improvement in predicting reattachment location by the modified ASM.

Wall Static-Pressure Distributions

Distribution of measured wall static pressure for both the step-side wall and opposite wall are shown in Fig. 3. A one-dimensional inviscid flow solution and calculations by Sindir are also shown. First, the data show that through the recirculating region, pressure along the step-side wall behaves nothing like that of a one-dimensional inviscid flow solution. Also evident from the measurements is the influence of separation on the flow upstream of the step. Beyond 8 step-heights downstream of reattachment, the pressure distribution becomes uniform across the tunnel, suggesting that boundary-layer assumptions will hold.

One noticeable difference in the two cases is the difference in the wall static-pressure gradient in the vicinity of reattachment. The maximum streamwise pressure gradient along the opposite wall for the undeflected-wall case ($HdC_p/dx = 0.006$) is substantially less than for the deflected-wall case ($HdC_p/dx = 0.015$). The pressure distribution along the step-side wall, however, exhibits a steeper pressure gradient in the vicinity of reattachment for the undeflected-wall case. In both cases, the significant portion of the pressure rise takes place ahead of reattachment.

Calculations for the step-side wall (shown in Fig. 3) demonstrate the premature pressure rise by the k-ϵ models and the standard ASM. The ASM (mod-ϵ) is seen to do quite well.

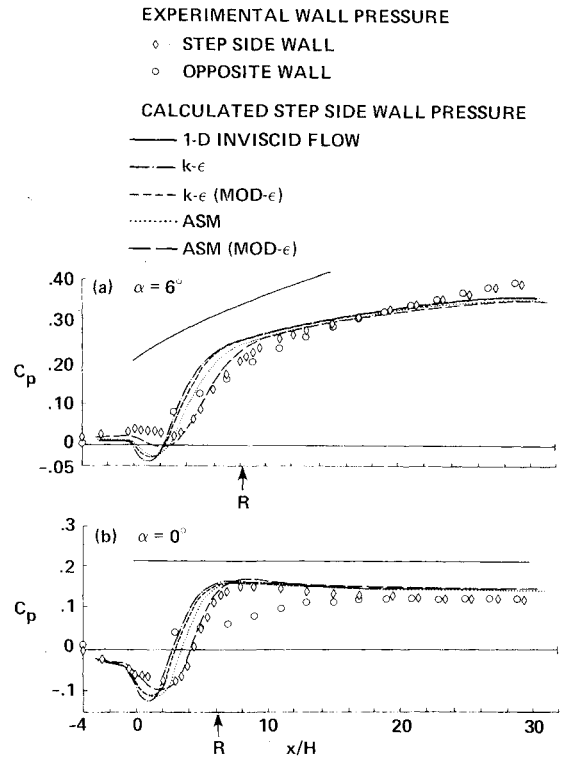

Fig. 3 Wall static pressure distribution.

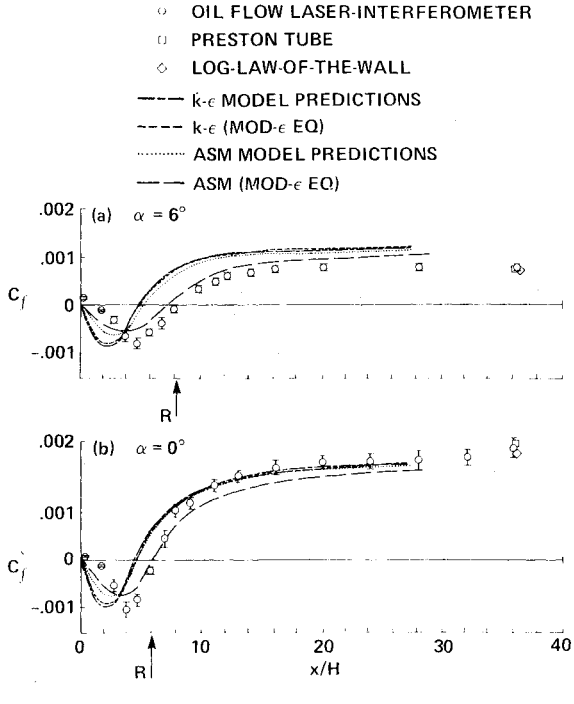

Fig. 4 Skin-friction distributions.

Skin-Friction Data

Measurements of step-side wall skin friction, using the oil flow laser interferometer, are shown in Fig. 4. Also shown are measurements by Preston tube and log-law-of-the-wall velocity profiles in the attached boundary-layer region well downstream of reattachment. These agree very well with the results from the oil flow laser interferometer. Sindir's calculations are also shown.

The measurements show high levels of skin friction in the reversed flow region, an indication of the energetic mixing

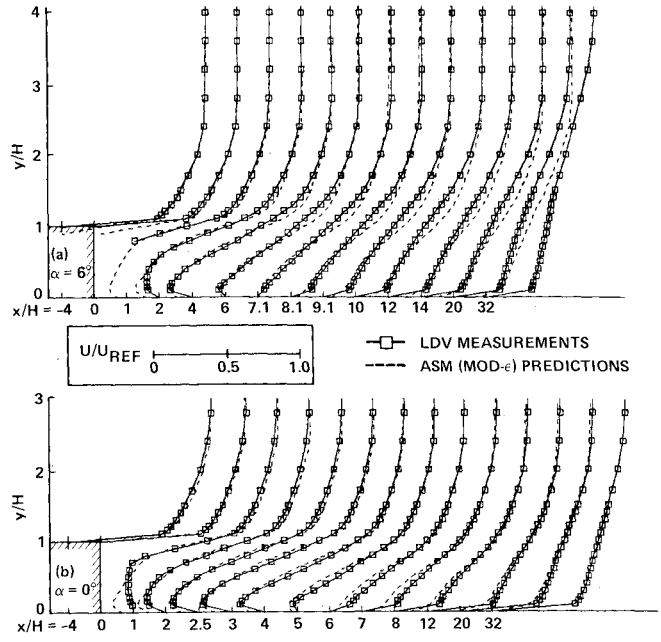

Fig. 5 Mean-velocity profiles in the separated and reattached regions.

producing extremely steep velocity gradients near the wall. Tunnel wall divergence is seen to reduce the levels of skin friction in the reattached flow, as well as in the separated regions of the flow. Also seen in the measurements is the presence of a small corner eddy confined to within 2 step-heights of the step. Skin-friction measurements ahead of the step (not shown) demonstrate the influence of separation on the flow ahead of the step.

Although each of the four turbulence models does a good qualitative job of predicting the flow, the modified ASM shows improvement over the other models.

Mean Velocity Data

Streamwise velocity measurements acquired by the LDV are shown in Fig. 5 for the two test cases. The velocity predictions obtained using an ASM (mod-ε) are also shown.

In both cases, the data show that the velocity gradient is nearly constant across the shear layer. Also, velocity measurements near the wall indicate an early reattachment relative to measurements by either skin friction or thermal tufts. This is perhaps an indication that the flow reversal is confined to a long, thin region in the downstream portion of separation. Moreover, it is not until quite far downstream of reattachment ($X/H > 16$) that the measured velocity profiles near the wall show any evidence of a log-law-of-the-wall region. This may be an indication of the existence of small length scales near the wall.

Predictions by the ASM (mod-ε) show quite good agreement with the data.

Turbulent Reynolds Stresses

Three components of turbulent Reynolds stresses ($\langle u^2 \rangle$, $\langle v^2 \rangle$, and $\langle uv \rangle$) were measured with the LDV. The two measured normal stresses ($\langle u^2 \rangle$ and $\langle v^2 \rangle$) exhibit the same overall behavior and will not be shown individually. Instead, the two-component turbulent kinetic energy $[(\langle u^2 \rangle + \langle v^2 \rangle)/2]$ is shown in Fig. 6. Also shown is the two-component turbulent kinetic energy calculated using the ASM (mod-ε). The turbulent shear stress ($-\langle uv \rangle$) is shown in Fig. 7. Sindir's shear-stress calculations are also shown.

In both test cases, the measured shear-stress and the kinetic energy demonstrate the features of a free shear layer, for example, a sudden increase in energy and shear soon after the step, followed by a steady increase through 5 step-heights

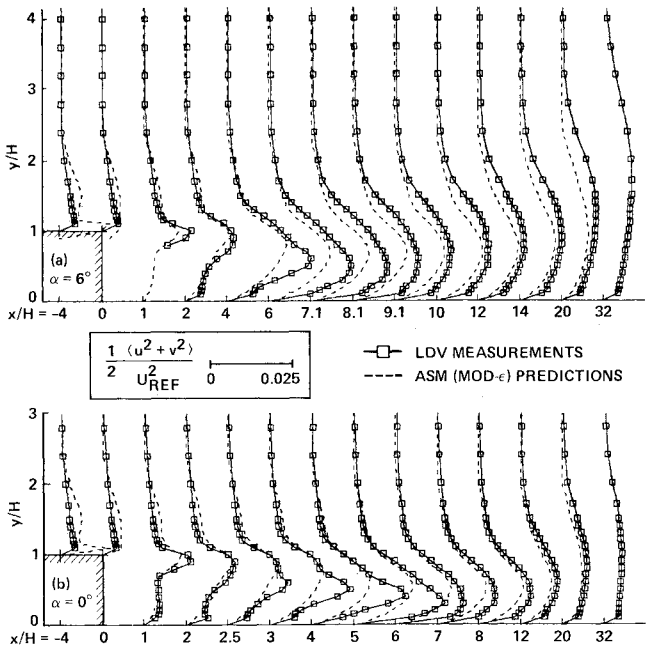

Fig. 6 Turbulent kinetic-energy profiles in the separated and reattached regions.

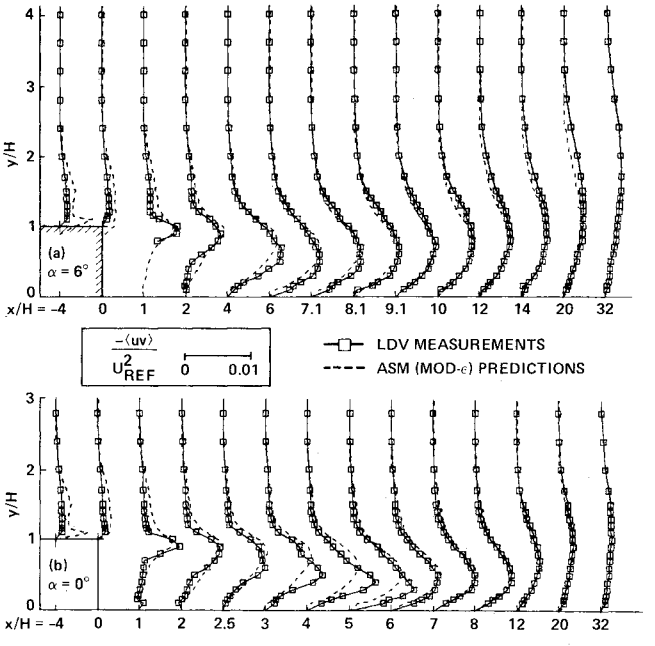

Fig. 7 Turbulent shear-stress profiles in the separated and reattached regions.

downstream of the step. From 5 step-heights on, the kinetic energy and shear-stress decay. In contrast to the free shear layer, the wall-side of the shear layer contains high levels of turbulent kinetic energy and shear-stress.

Differences are noted in the two cases of wall divergence. A higher level of kinetic energy and turbulent shear-stress in the reattached portion of the flow is noted in the divergent wall case. This may be due to a higher rate of production from the more distorted mean velocity profile. Turbulent kinetic energy and shear-stress tend to diffuse and convect farther into the freestream in the divergent wall case.

The calculations using the ASM (mod-ϵ) are quite good overall, but the peak values of kinetic energy and shear-stress tend to be somewhat displaced from the locations of peaks

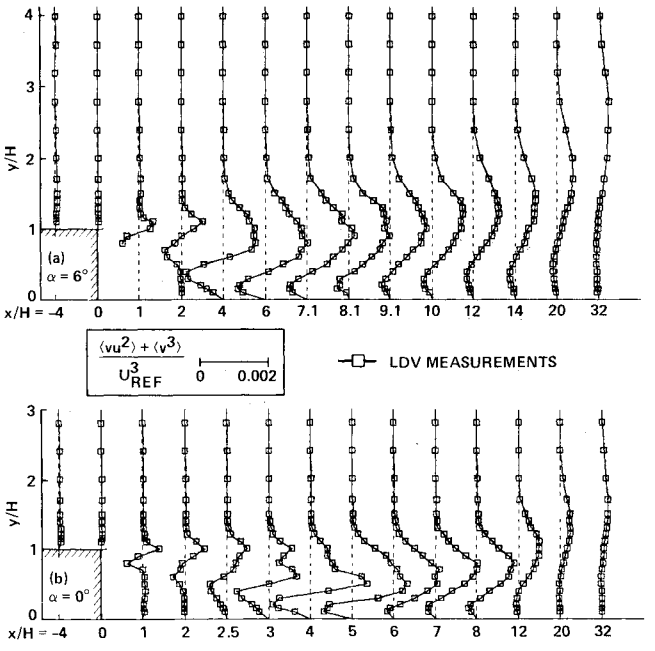

Fig. 8 Turbulent triple-product correlation profiles in the separated and reattached regions.

determined experimentally. One would expect the turbulent stress and kinetic energy to be convected along streamlines of the flow, as is the case in the experimental results. The numerical calculations appear to have trouble convecting the turbulent kinetic energy and shear-stress. Also, comparisons of the unmodified k-ϵ turbulence model and the unmodified ASM with the data (not shown) demonstrates Sindir and Launder's early findings that the models tend to overpredict the levels of shear-stress and kinetic energy.

Triple Products

The turbulent triple products that were measured are $\langle u^3 \rangle$, $\langle uv^2 \rangle$, $\langle vu^2 \rangle$, and $\langle v^3 \rangle$. The sum of the $\langle vu^2 \rangle$ and $\langle v^3 \rangle$ triple products is shown in Fig. 8. The other triple products $\langle u^3 \rangle$ and $\langle uv^2 \rangle$ were opposite in sign, but exhibited the same overall features. Again, the triple products exhibit the features of a free shear flow in the early stages of separation. They are antisymmetric about the centerline of the shear layer, reaching peak values to either side of the centerline of the shear layer and tapering off to zero at the edges of the shear layer. The triple-product correlations are seen to be virtually zero in the chaotic separated flow, as might be expected. However, the data show one major difference between the free shear layer and the reattaching shear layer: As Chanrusuda and Bradshaw first noticed,[14] the triple products on the wall side of the shear layer diminished rapidly upon approaching reattachment. One theory is that large eddies (the source of the triple-product correlations) are split in half by the wall at reattachment, annihilating the correlations. Turbulence models do not attempt to calculate triple-product correlations, and thus no predictions are shown.

Displacement and Momentum Thickness

To determine displacement and momentum thicknesses, the U-velocity profiles were integrated with respect to the Y direction using Simpson's rule. Cole's universal velocity profiles[15] were used for the region from the wall to the first point in the profile. Displacement and momentum thicknesses are shown in Fig. 9. The sudden displacement of the flow owing to the step is similar in both cases. One noticeable difference is that the flow does not recover from the displacement of the step for the divergent wall case as well as it does for the parallel wall case. The momentum thickness also undergoes a

larger increase in the divergent wall case. Additionally, in the case of wall divergence, the shape factor of (δ^*/θ) is slower to recover to a value of 1.4 (typical of an attached boundary layer).

Kinetic Energy Equation Balance

In order to calculate turbulent fluid flow, the equations of motion are typically time-averaged. The time-averaged equations still contain the usual unknowns (average velocities, density, and pressure), but unfortunately they also contain terms arising from the turbulent fluctuations (Reynolds stresses). The problem is that while creating more unknowns, there is still the same number of equations. To overcome this problem, some turbulence modelers derive and solve equations that govern the transport of production and dissipation of turbulent kinetic energy in addition to the original time-averaged equations of motion. Kinetic energy and dissipation are typically combined in a Boussinesq approximation or algebraically to obtain the Reynolds stresses.

The equation of kinetic energy is derived in Ref. 16 and can be written as

$$U\frac{\partial k}{\partial x} - V\frac{\partial k}{\partial y} = -\left[\frac{\partial \overline{up}}{\partial x}\right] - \frac{\partial \overline{uk}}{\partial x} - \left[\frac{\partial \overline{vp}}{\partial y}\right] - \frac{\partial \overline{vk}}{\partial y} - \overline{uv}\frac{\partial U}{\partial y}$$

$$+\left(\overline{u}^2 - \overline{v}^2\right)\frac{\partial U}{\partial x} - \epsilon$$

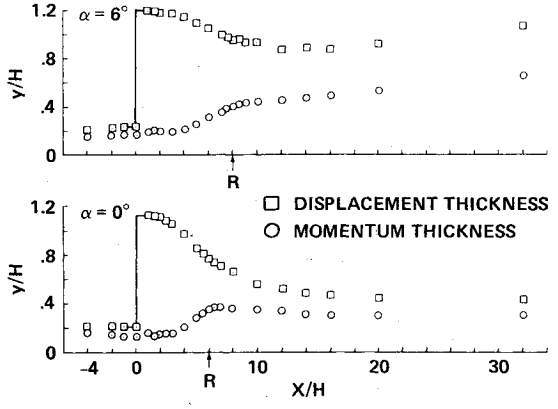

Fig. 9 Variation of boundary-layer integral thickness parameters.

Using the assumption that values of $\langle w^2 \rangle$ lie midway between $\langle u^2 \rangle$ and $\langle v^2 \rangle$, the kinetic energy (k) can be approximated by $3/4(\langle u^2 \rangle + \langle v^2 \rangle)$, enabling convection (first and second terms) to be determined from the data. Similarly, the turbulent diffusion (fourth and sixth terms) can be determined if $\overline{uk}$ and $\overline{vk}$ are approximated by $3/4(\langle u^3 \rangle + \langle uv^2 \rangle)$ and $3/4(\langle vu^2 \rangle + \langle v^3 \rangle)$, respectively. The production (seventh and eighth terms) can be computed exactly from the data. Differentiation is done by central difference. Pressure diffusion (third and fifth) terms are presumed to be small and are neglected. The dissipation (ninth term) can be inferred by balancing the equation. The energy-balance terms are shown in Figs. 10-12 for stations of 2.1 step-heights upstream of reattachment and 1.9 and 5.9 step-heights downstream of reattachment. The calculations of production and dissipation, made using the modified and unmodified k-ϵ and algebraic-stress turbulence models are also shown.

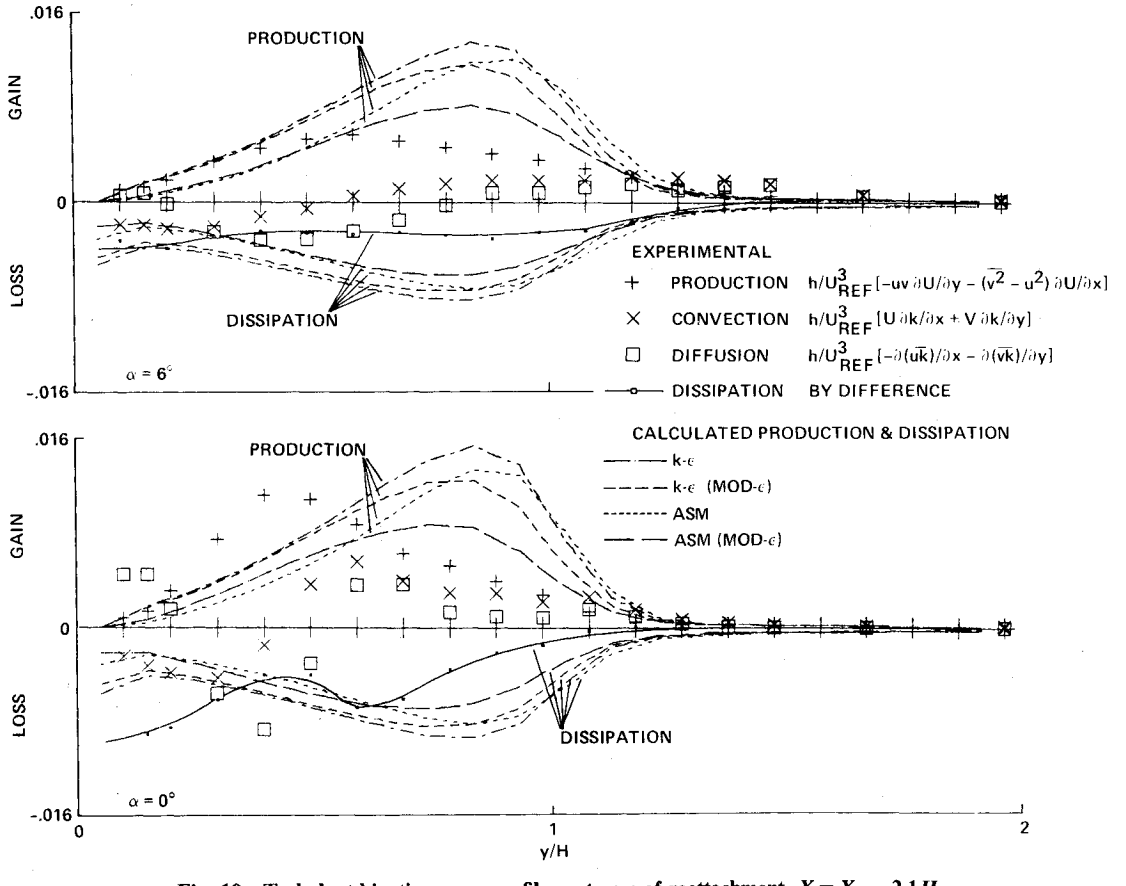

Fig. 10 Turbulent kinetic-energy profile upstream of reattachment, $X = X_R - 2.1H$.

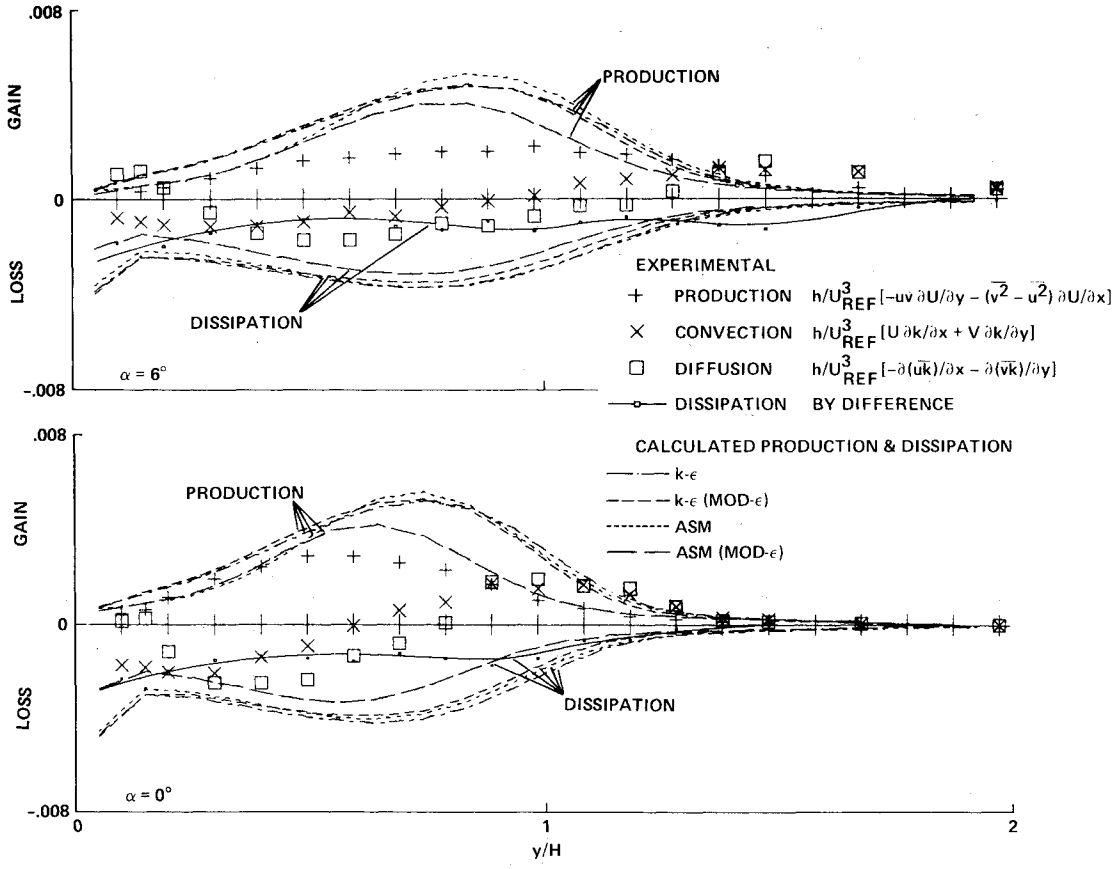

Fig. 11 Turbulent kinetic-energy balance downstream of reattachment, $X = X_R + 1.9H$.

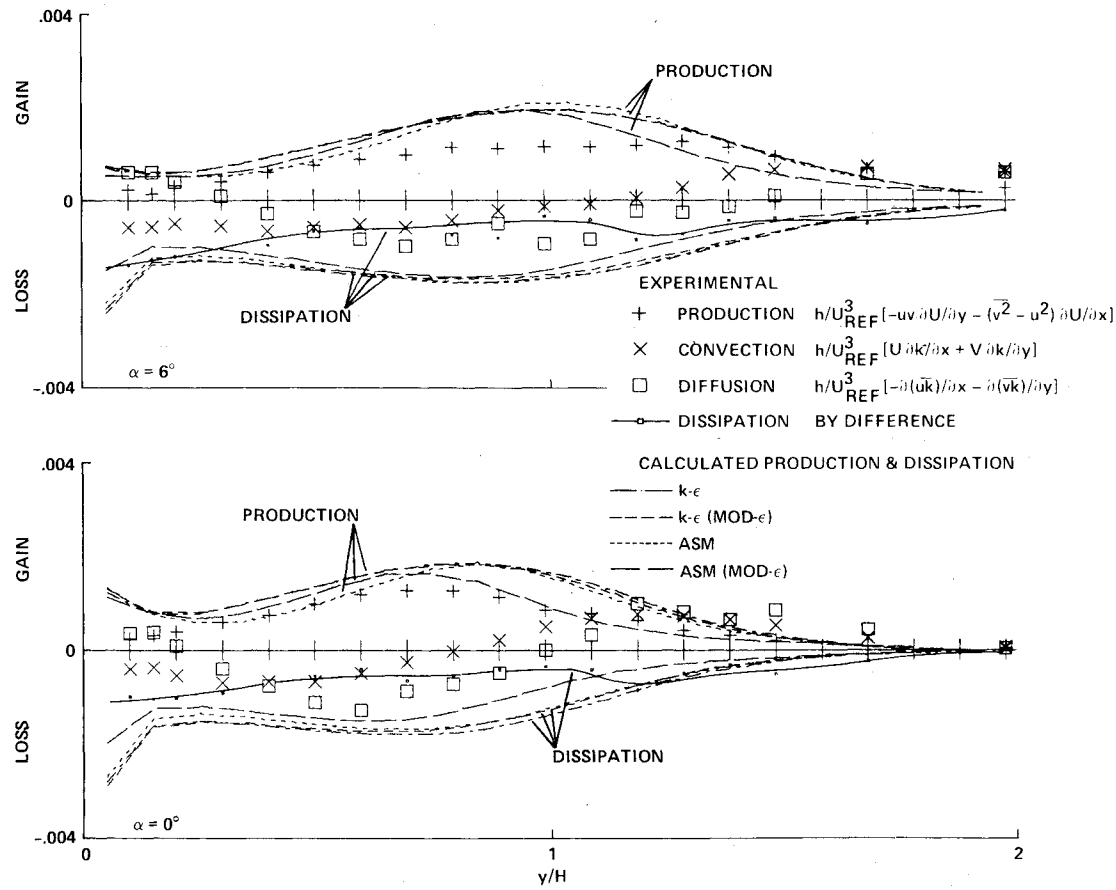

Fig. 12 Turbulent kinetic-energy balance profile far downstream of reattachment, $X = X_R + 5.9H$.

The data demonstrate that convection and diffusion significantly contribute to the kinetic energy balance. The data show that the dissipation is substantially less than production through the central portion of the shear layer. This may be a consequence of the large eddies produced at separation not having had time to break up into smaller dissipative eddies before being convected downstream and diffused. Throughout the outer part of the shear layer, turbulent diffusion behaves similarly to convection (a standard turbulence modeling assumption), but diffusion in the separated bubble and near the wall behaves altogether differently. The diffusion goes positive again and convection stays negative. Although all terms are smaller in the case of divergent walls, their relative importance has not changed significantly. The wall divergence producing lower dissipation rates, combined with the high level of kinetic energy, is an indication of larger length scales and eddy viscosities, which will be made apparent in the following sections.

The calculations using the four different turbulence models consistently overpredict the dissipation rate and production of turbulent kinetic energy. The ASM (mod-ϵ), although it does a better job of predicting production, does not significantly improve on the predictions of dissipation rate. Perhaps more constructive to turbulence modeling effort is the point that numerically calculated dissipation rate is quite high relative to numerically calculated production through the central portion of the shear layer, an indication that the model for diffusion in the kinetic energy equation may be inadequate. In addition to these difficulties, the models tend to be insensitive to wall divergence effects on the production and dissipation of kinetic energy.

Eddy Viscosity

Figure 13 shows the experimental eddy viscosity as determined by

$$\nu_t = \frac{-\langle uv \rangle}{dU/dy + dV/dx}$$

Also shown are eddy viscosities predicted by the Cebeci-Smith[17] turbulence model for the outer flow, determined by

$$\nu_t = 0.016\left(U_e\delta^*/\nu_m\right)/\left[1.0 + 5.5(y/\delta)^6\right]$$

and by the Jones-Launder[18] turbulence model (using the experimentally determined values of dissipation and kinetic energy) given by

$$\nu_t = 0.09k^2/\epsilon$$

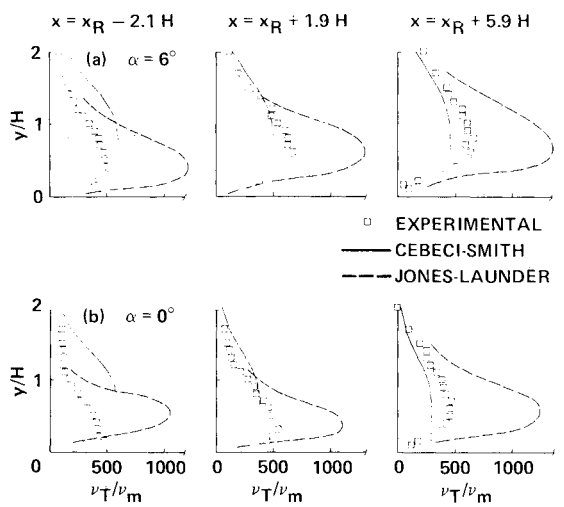

Fig. 13 Eddy-viscosity profiles in the reattachment region.

The data show a steady increase in eddy viscosity with distance from separation: beyond reattachment the eddy viscosity levels off to near-constant peak values. Wall divergence only slightly increases the peak values of eddy viscosity. The data demonstrate a difficulty with the Cebeci-Smith turbulence model, which is predicting a decrease in eddy viscosity with distance from separation contrary to what the data show. The Jones-Launder model tends to overpredict the eddy viscosity, which may be an explanation for it predicting too high a spreading rate for the shear layer and thus a premature reattachment.

Conclusions

In the interest of understanding the physics of turbulence and to guide turbulence modeling, a detailed experiment has been done on a reattaching shear layer in a rearward-step flow with wall divergence. The experiment was performed at a high Reynolds number in an incompressible flow. The mean and turbulent fluctuations in the flowfield have been measured with a laser Doppler velocimeter, and skin friction was measured with a nonintrusive laser interferometer for two cases.

The main features of a reattaching shear flow in the presence of wall divergence can be summarized as follows.

1) The wall divergence increases the spreading rate of the shear layer, lengthens reattachment, and delays pressure recovery, while increasing the momentum and displacement thicknesses.

2) There are no major differences in the Reynolds stresses between the two cases of wall divergence. In both cases, Reynolds stresses grow in a similar way to nearly the same peak values. They decay in a similar way in either case, with the exception that wall divergence sustains a higher value of Reynolds stresses after reattachment.

3) Turbulent triple-product correlation on the wall-side of the shear layer are abruptly annihilated at reattachment. This phenomenon is similar in both cases.

4) Comparisons with the data show that the modifications of the algebraic-stress model substantially improved numerical calculations over calculations using the unmodified k-ϵ and algebraic-stress models. The same modification had little or no effect on the predictions by the standard k-ϵ model. Although all models showed good qualitative agreement with the data, only the modified ASM gave results adequate for engineering practice. One noticeable difficulty with all models is their inability to locate the peak of turbulent Reynolds stresses. This may be a result of inadequate treatment of either convection or diffusion in the kinetic energy transport equation.

5) Although production and dissipation remain the dominant mechanisms in the kinetic energy equation, there are significant contributions by the diffusion and convection terms. Wall divergence tends to decrease the mechanisms of production, dissipation, diffusion, and convection of turbulent kinetic energy. The algebraic-stress model and the k-ϵ model consistently overpredict the levels of dissipation in the shear layer, perhaps pointing to a difficulty with the dissipation rate equation.

6) The eddy viscosities predicted by a zero-equation eddy-viscosity model demonstrate a decrease in eddy viscosity with distance from separation, the opposite trend to what the data show. The Jones-Launder eddy-viscosity assumption, although holding quite well in general, appears to overestimate the eddy viscosity in the central part of the shear layer.

Acknowledgments

We are thankful to Dr. Munir Sindir and Dr. Brian Launder for providing the results of algebraic-stress model and k-ϵ model predictions. We are also deeply indebted to Mr. D. Harrison for the design and development of the LDV electronics and computer interfacing hardware, and to Dr. J. L. Brown for pioneering the software for performing the data acquisition. We would also like to thank Community College students K. Davis and G. Switzer for their invaluable help.

References

[1]Eaton, J. and Johnston, J., "A Review of Research on Subsonic Turbulent-Flow Reattachment," *AIAA Journal*, Vol. 19, Sept. 1980, pp. 1093-1100.

[2]Eaton, J.M.K., "Summary of Computations for Predictive Cases—Modified Backward-Facing Step Flows," 1980-81 AFSOR-HTTM-Stanford Conference on Complex Turbulent Flows: Comparison of Computation and Experiments, Stanford University, Stanford, Calif., 1981.

[3]Kuehn, D.M., "Some Effects of Adverse Pressure Gradient on the Incompressible Reattaching Flow over a Rearward-Facing Step," *AIAA Journal*, Vol. 18, March 1980, pp. 343-344.

[4]DeBredorod, V. and Bradshaw, P., "Three-Dimensional Flow in Nominally Two-Dimensional Separation Bubbles. I. Flow Behind a Rearward-Facing Step," I. C. Aero Report 72-19, Aug. 1972.

[5]Badri Narayanan, M., Khadge, Y., and Viswanath, P., "Similarities in Pressure Distribution in Separated Flow Behind Backward-Facing Steps," *Aeronautical Quarterly*, Vol. 25, Pt. 4, Nov. 1974, pp. 305-312.

[6]Monson, D., Driver, D., and Szodruch, J., "Application of a Laser Interferometer Skin-Friction Meter in Complex Flows," *ICIASF'81 Record*, International Congress on Instrumentation in Aerospace Simulation Facilities, Oct. 1981, pp. 232-243.

[7]Monson, D. and Higuchi, H., "Skin Friction Measurements by a Dual-Laser-Beam Interferometer Technique," *AIAA Journal*, Vol. 19, June 1981, pp. 739-744.

[8]Westphal, R.V., Eaton, J.K., and Johnston, J.P., "A New Probe for Measurement of Velocity and Wall Shear Stress in Unsteady, Reversing Flow," *Journal of Fluids Engineering*, Vol. 103, Sept. 1981, pp. 478-482.

[9]Seegmiller, H.L., et al., "Application of Laser Velocimetry to an Unsteady Transonic Flow," *ICIASF'79 Record*, International Congress on Instrumentation in Aerospace Simulation Facilities, Sept. 1979, pp. 284-293.

[10]Driver, D.M. and Seegmiller, H.L., "Features of a Reattaching Turbulent Shear Layer Subject to an Adverse Pressure Gradient," AIAA Paper 82-1029, June 1982.

[11]Gosman, A., Pun, M.W., Runchal, A., Spaulding, D., and Wolfstein, M., *Heat and Mass Transfer in Recirculating Flows*, Academic Press, London, 1969.

[12]Kim, J., Kline, S., and Johnston, J., "Investigations of Separation and Reattachment of a Turbulent Shear Layer: Flow over a Backward-Facing Step," Thermosciences Division, Dept. of Mechanical Engineering, Stanford Univ., Stanford, Calif., Rept. MD-37, April 1978.

[13]Sindir, M., "Numerical Study of Separating and Reattaching Flows in a Backward-Facing Step Geometry," Doctoral dissertation, Mechanical Engineering, University of California at Davis, Calif., 1982.

[14]Chanrusuda, C. and Bradshaw, P., "Turbulence Structure of a Reattaching Mixing Layer," *Journal of Fluid Mechanics*, Vol. 110, 1981, pp. 171-194.

[15]Coles, D., "The Young Person's Guide to the Data," Computation of Turbulent Boundary Layer—1968, AFOSR-IFP-Stanford Conference, Vol. II, Thermosciences Div., Dept. of Mechanical Engineering, Stanford Univ., Stanford, Calif., 1969.

[16]Tennekes, H. and Lumeley, J., *A First Course in Turbulence*, The MIT Press, Cambridge, Mass., 1972.

[17]Cebeci, T. and Smith, A.M.O., *Analysis of Turbulent Boundary Layers*, Academic Press, New York, 1974.

[18]Jones, W.P. and Launder, B.E., "The Prediction of Laminarization with a 2-Equation Model of Turbulence," *International Journal of Heat and Mass Transfer*, Vol. 15, Feb. 1972, pp. 301-304.